

Synthesis and Adsorption Application of In Situ Photo-Cross-Linked Electrospun Poly(Vinyl Alcohol)-Based Nanofiber Membranes

Bihter Zeytuncu · Süleyman Akman · Onuralp Yucel · Memet Vezir Kahraman

Received: 24 October 2014 / Accepted: 26 January 2015 / Published online: 9 May 2015
© Springer International Publishing Switzerland 2015

Abstract Poly(vinyl alcohol)/maleic anhydride/acryloyl thioamide monomer (PVA/MA/ATM) nanofiber membranes (NFm) were synthesized by a combination of UV radiation and an electrospinning technique. The PVA/MA/ATM NFm were characterized by Fourier transform infrared spectroscopy (FT-IR), thermogravimetric analysis (TGA), Brunauer–Emmert–Teller (BET) analysis, scanning electron microscopy (SEM), and energy dispersion spectrometry (EDS). These membranes were used for adsorption–desorption of platinum (Pt(IV)) and palladium (Pd(II)) from a fire assay (FA) leaching waste solution, and the effect of process parameters such as pH of solution, contact time, NFm dosage, temperature, and adsorption isotherms and kinetics studies on the recovery of Pt(IV) and Pd(II) from the waste solution were investigated. The adsorption equilibrium data fit better using the Langmuir model than the Freundlich

model. Maximum adsorption capacities, Q_{\max} , at 45 °C were found to be 69.93 and 112.36 mg/g for Pt(IV) and Pd(II), respectively. The activation energies (E_a) of Pt(IV) and Pd(II) were 27.90 and 20.29 kJ/mol, respectively. The best desorption reagent was a 1.0 M HCl–1.0 M thiourea (TU) solution for both Pd(II) and Pt(IV). Reusability studies showed that the adsorption capacity can remain up to 90 % after five times of usage. This study provides a promising NFm with an effective adsorption property for Pt(IV) and Pd(II) ions.

Keywords Electrospinning · Nanofiber · Thioamide · Adsorption · Platinum · Palladium

1 Introduction

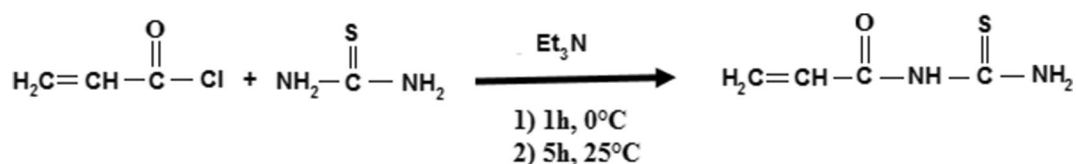
Since mid 1990s, many researchers have investigated electrospinning techniques and electrospun nanofiber materials. Fiber with a diameter range of 20–2000 nm is named as nanofiber and can be achieved by the electrospinning technique, which is the most effective method of applying high voltage on a polymer solution (Reneker and Yarin 2008). Electrospun nanofiber membranes have a wide range of applications for use, such as in drug-delivery systems (Tonnesen and Karlsen 2002; Kenawy et al. 2002), scaffolds in tissue engineering (Cakmakci et al. 2012; You et al. 2005), clothing protection (Gibson et al. 2001), sensors (Aussawasathien et al. 2005) and fine filtration, and adsorptive membranes (Aliabadi et al. 2013; Ramakrishna et al. 2006; Ma et al. 2006; Neghlani et al. 2011). These applications

B. Zeytuncu (✉)
Applied Research Center of Materials Science and Production
Technology, Istanbul Technical University, 34469 Istanbul,
Turkey
e-mail: bihter_zeytuncu@hotmail.com

S. Akman
Faculty of Science and Letters, Department of Chemistry,
Istanbul Technical University, 34469 Istanbul, Turkey

O. Yucel
Faculty of Chemical and Metallurgical Engineering, Istanbul
Technical University, 34469 Istanbul, Turkey

M. V. Kahraman
Faculty of Science and Letters, Department of Chemistry,
Marmara University, 34722 Istanbul, Turkey



Scheme 1 Proposed structure of the synthesized acryloyl thioamide monomer (ATM)

are achievable because nanofiber membranes show numerous interesting characteristics such as high porosity, small pore size, and—most importantly—a high specific surface area (Reneker and Yarin 2008; Huang et al. 2003). Based on the above properties, nanofiber membranes have been speculated to have a high adsorption capacity. The introduction of specific functional groups onto the electrospun nanofibers has also been reported for the recovery of specific materials from waste/aqueous solutions (Feng et al. 2011; Teng et al. 2011).

The recent literature has included several methods for the recovery of precious metals (i.e., platinum, palladium, rhodium, ruthenium, osmium, iridium, gold, and silver) from aqueous solutions, such as solvent extraction (Shamsipur et al. 2009; Hung et al. 2007), ion-exchange (Shen et al. 2010; Godlewska-Żylkiewicz et al. 2000; Shen et al. 2011), filtration (Li et al. 2013; Trivunac and Stevanovic 2006; Borbély and Nagy 2009), cementation (Aktas 2012; Morcali et al. 2013a), and adsorption (Wang et al. 2011; Kyzas et al. 2013; Morcali et al. 2013b). Among these methods, adsorption is the most suitable method for the recovery of precious metals due to its low cost, ease in handling, high efficiency, reversibility, and the availability of different adsorbents. A number of adsorbents have been developed for the recovery of precious metals, such as activated carbon (Navarro et al. 2006; Aktas and Morcali 2011a), chelating

resins (Atia et al. 2005; Birinci et al. 2009), and membranes (Fayemi et al. 2013). The adsorption efficiency, selectivity, equilibrium time, regeneration, and stability of these materials depend on the functional groups of the adsorbent surface, which are effective in forming complexation with metal ions.

The adsorbents with functional groups that include sulfur and nitrogen donor atoms are very efficient at chelating with soft metal ions. According to the hard–soft acid–base (HSAB) theory by Pearson (1963), soft metal ions, such as gold, silver, platinum, and palladium ions, show an affinity to soft bases with donor atoms as $\text{O} < \text{N} < \text{S}$ (Pearson 1963). Therefore, recent research has focused on the synthesis of novel materials that contain donor atoms for the adsorption of precious metals (Li et al. 2013; Fırlak et al. 2013; Lin and Lien 2013).

Poly (vinyl alcohol) (PVA) is a water-soluble, non-toxic, and biocompatible polyhydroxy polymer, with good chemical and thermal stability. PVA is known to easily interact with other organic and inorganic materials (Islam and Karim 2010). However, applications of PVA are limited because of its hydrophilicity. Thus, PVA must be modified to minimize swelling in water when fabricated for especially aqueous applications (Wu et al. 2010a, b; Sasipriya et al. 2013). Chemical cross-linking by dialdehydes, dicarboxylic acids, or dianhydrides is advantageous because it renders the nanofibers insoluble in all solvents and increases the thermal and chemical properties of the membranes (Bolto et al. 2009; Yang et al. 2008).

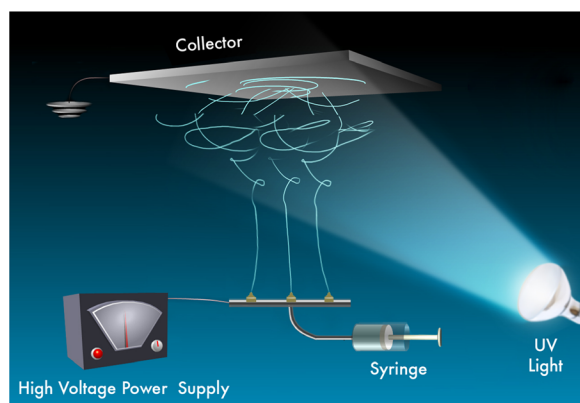


Fig. 1 The schematic diagram of electrospinning process combined with UV radiation

Table 1 Element concentrations in the fire assay leaching solution

Element	Concentration (mg/L)
Pt	29.79
Pd	44.19
Rh	3.86
Ru	0.05
Au	0.01
Pb	2.79
Cu	0.28
Ni	1.04
Zn	0.26

In the present study, in situ photo-cross-linked electrospun nanofiber membranes containing thioamide groups were synthesized and applied for the adsorption of platinum and palladium ions from aqueous system. The structure and surface morphology of PVA/MA/ATM NFMs were analyzed by Fourier transform infrared spectroscopy (FT-IR), scanning electron microscopy (SEM), and energy dispersion spectrometry (EDS). Adsorption isotherms and kinetic calculations for the adsorption process are also reported. Finally, the reusability of the PVA/MA/ATM NFm was determined after five adsorption–desorption cycles.

2 Material and Methods

2.1 Materials

PVA (87–89 % hydrolyzed, M_w 146,000–186,000 g/mol), maleic anhydride (MA), acryloyl chloride, and the radical photoinitiator, 2-hydroxy-2-methyl-1-phenyl-1-propan-1-one (Darocur® 1173), were purchased from Aldrich-Sigma. Thiourea (TU), triethylamine (TEA), and dimethylformamide (DMF) were purchased from Merck. Water was deionized using a water

purification system (TKA, Germany) to a resistance of 18.2 M Ω cm before preparing all of the solutions.

2.2 Characterization

The infrared spectrum of prepared membranes was obtained with a FT-IR spectrometer (Spectrum 100, PerkinElmer, USA) in the wave number region of 4000–400 cm^{-1} to define the characteristic peaks of the functional groups of the nanofiber membranes. Thermogravimetric analysis (TGA) studies were carried out using a PerkinElmer Thermogravimetric Analyzer Pyris 1 TGA model at a heating rate of 10 $^{\circ}\text{C}/\text{min}$ in air atmosphere, over a temperature range from room temperature to 700 $^{\circ}\text{C}$. The surface morphology of nanofiber was examined with SEM-EDS (JEOL JSM 7000F). The surface area of nanofiber membrane was determined using BET analysis (ASAP 2020).

2.3 Preparation of Precursor sol

First, acryloyl thioamide monomer (ATM) was synthesized with a reaction between acryloyl chloride and thiourea (TU). TU in 20-mL DMF and triethylamine (0.15 mol) was added into a 500-mL three-necked flask. Acryloyl chloride (0.15 mol) was slowly added dropwise

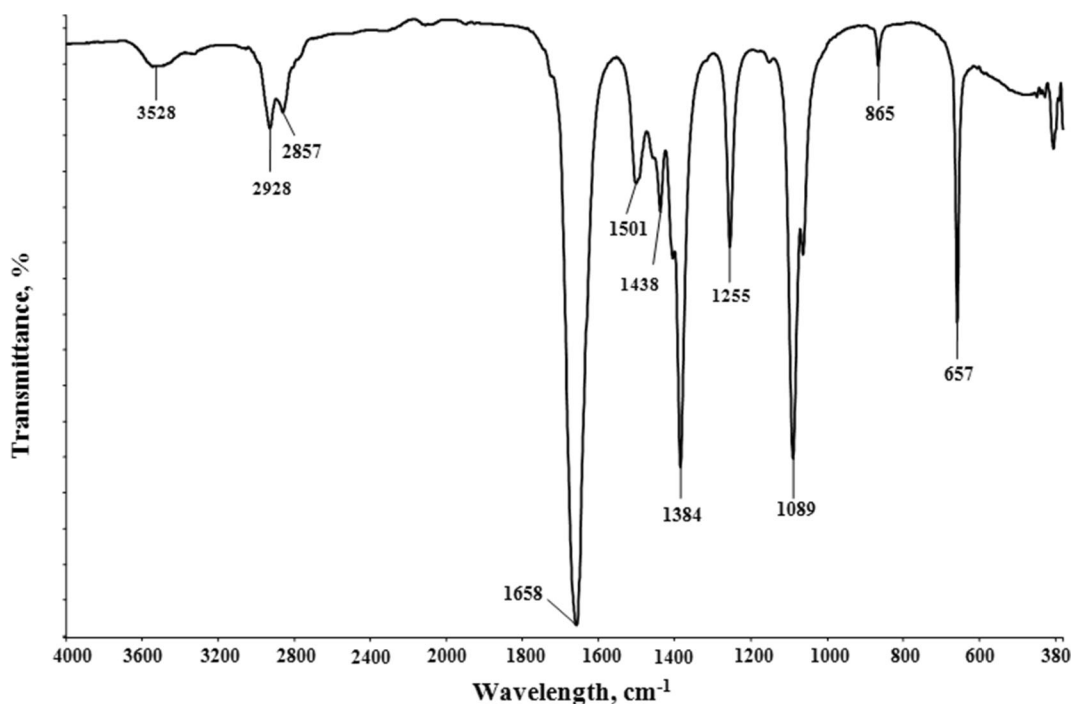


Fig. 2 The FT-IR spectrum of ATM

to the reaction mixture, while continuously stirring, at 0 °C under nitrogen atmosphere. After 1 h at 0 °C, the reaction continued at room temperature for an additional 1 h (Scheme 1). The solvent was evaporated. The synthesized ATM was dried in a vacuum oven at 30 °C overnight.

Second, a 10 % solution was prepared from PVA powder dissolved in distilled water. Then, maleic anhydride (MA) (0.98 g) was added into the solution in the presence of NaOH with vigorous stirring at 70 °C for 5 h for the esterification reaction to occur between PVA and MA. Then, ATM (1.00 g) was added into the cooled PVA/MA mixtures. Finally, Darocur® 1173 was added to the mixture (3 wt.%) and stirred until homogenation was achieved.

2.4 Synthesis of Nanofiber Membranes

The prepared sol was placed in a syringe. While the negative terminal was connected to a conductive drum

covered with aluminum foil as a collector of fibers, the positive terminal of a high-voltage power supply was connected to the metallic syringe tip. A voltage of 25 kV with a tip-to-target distance of 15 cm at a speed of 0.1 mL/h was applied to the solution, being irradiated with a high-pressure UV lamp ($\lambda_{\text{max}}=365$ nm, OSRAM 300 W) to provide polymerization of the jet during its flight and promoting the cross-linking of PVA/MA and ATM. The nanofiber membranes (NFm) were collected on the aluminum foil. The schematic diagram of electrospinning process combined with UV radiation is shown in Fig. 1. The synthesized NFm were dried for 12 h at 100 °C in an incubator. Then, they were refluxed in ethanol/HCl (molar ratio 10:1) for 24 h at 70 °C to remove excess monomer and then dried for 6 h at 30 °C in a vacuum.

2.5 Generation of Fire Assay Leaching Solution

The solutions were obtained by leaching the fire assay (FA) (i.e., NiS-FA and Pb-FA) bead in our university

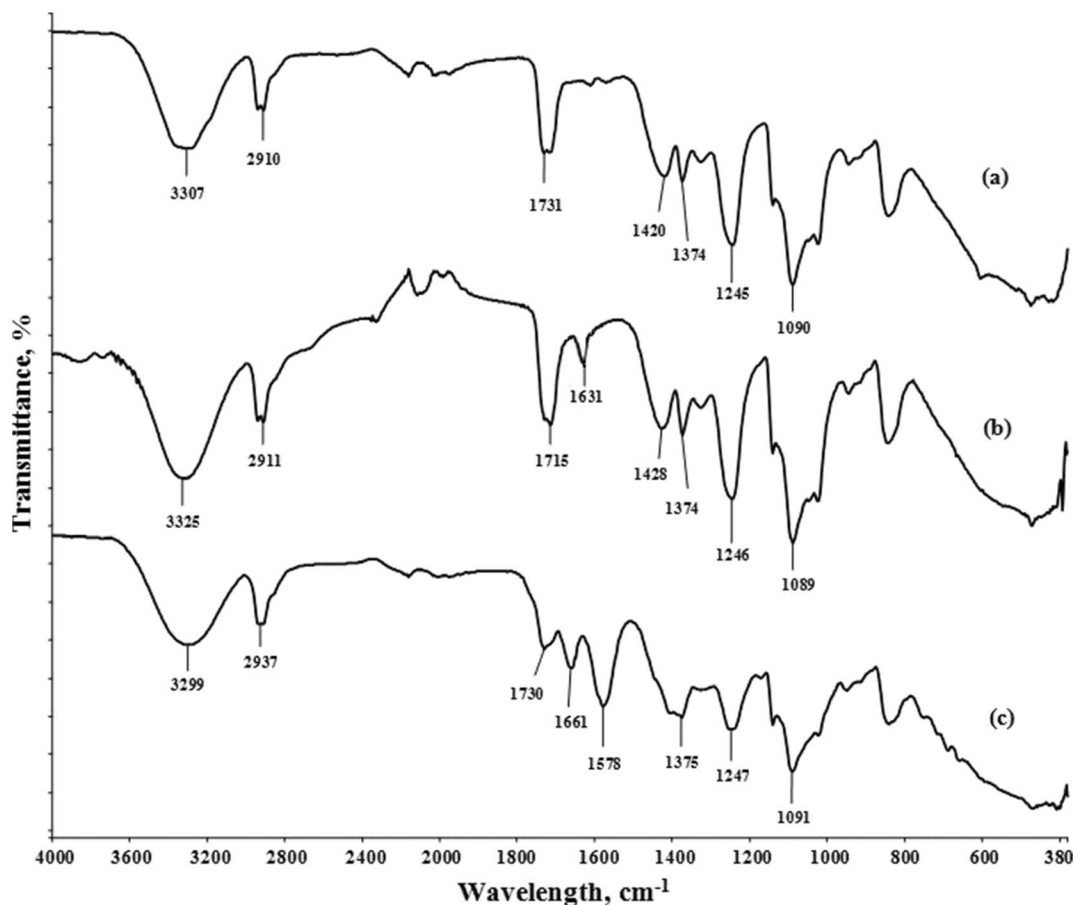


Fig. 3 FT-IR spectra of **a** PVA, **b** PVA/MA, and **c** PVA/MA/ATM NFm

laboratories. The bead that contained precious metals was dissolved with aqua regia (HCl/HNO₃ 3:1) (Morcali et al. 2014a). Finally, the solution was diluted to 2 L with distilled–deionized water. This was used in our adsorption experiments (Pt(IV), Pd(II)). The concentrations of all the main elements, which are denoted as initial concentrations, were measured by ICP-MS and are listed in Table 1. The leaching solution was a five-component system (with two major components being Pt and Pd and three minor ones as Rh, Pb, and Ni.)

The preliminary investigation of their adsorption on the PVA/MA/ATM NFm was carried out. The chloride solution of 50 mL was contacted with 250 mg of the resin for 5 h. After that, the sample was filtered without any washing, and the filtrate was used for analysis. The adsorption percentages of metal ions were expressed by the variation percentage of metal concentration. The adsorption percentages of Pt, Pd, and Rh were 51.61, 41.09, and 0.13 %, respectively, and the adsorptions of other ions (Ru, Au, Pb, Ni, Cu, and Zn) on the PVA/MA/ATM NFm were negligible.

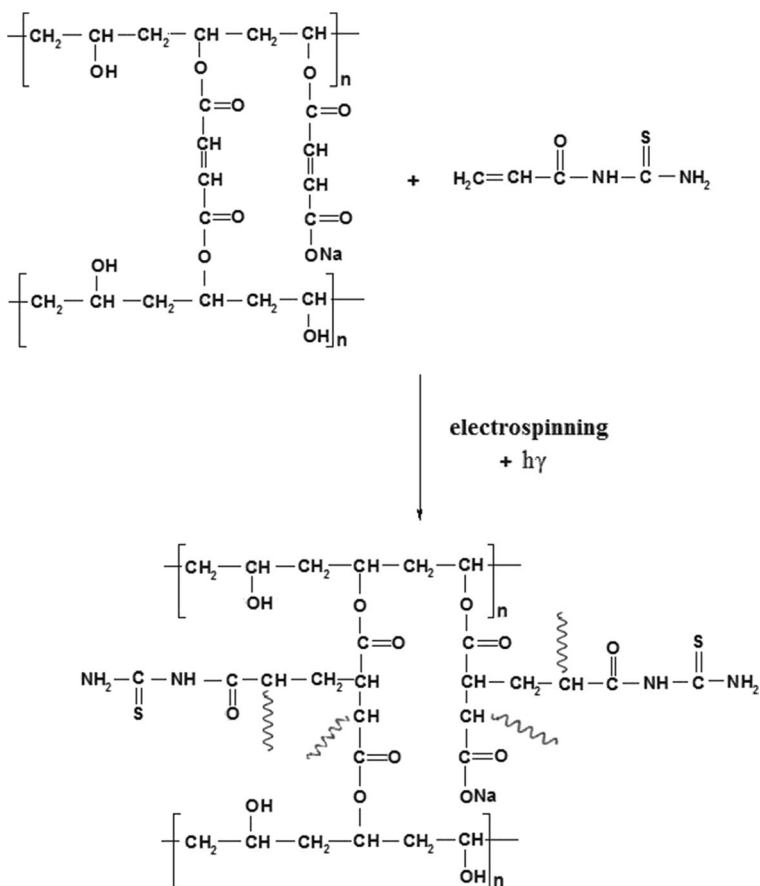
2.6 Adsorption Studies

The effect of solution pH on the PVA/MA/ATM NFm adsorption of Pt(IV) and Pd(II) using 150 mg of the NFm was investigated in 50 mL solution and the other parameters kept constant (e.g., 25 °C, 60 min and 600rpm).

The effect of varying the PVA/MA/ATM NFm dosage from 50 to 250 mg (i.e., 1 to 5 mg/mL) was investigated. For this experiment, 50 mL of the solution was brought into contact with the sorbent for 60 min at 25 °C and 600 rpm in a flask.

The effect of contact time on the PVA/MA/ATM NFm adsorption of Pt(IV) and Pd(II) using 100 mg of the NFm was investigated in a flask containing 100 mL of solution. The flasks were vigorously stirred on a magnetic stirrer at 25 °C and 600 rpm. Five milliliters of the solution was extracted at different time intervals to analyze the residual metal ion concentration in the solution. A similar procedure was utilized to test for the effect of temperature, which ranged from 25 to 45 °C.

Scheme 2 Proposed structure of the PVA/MA/ATM NFm



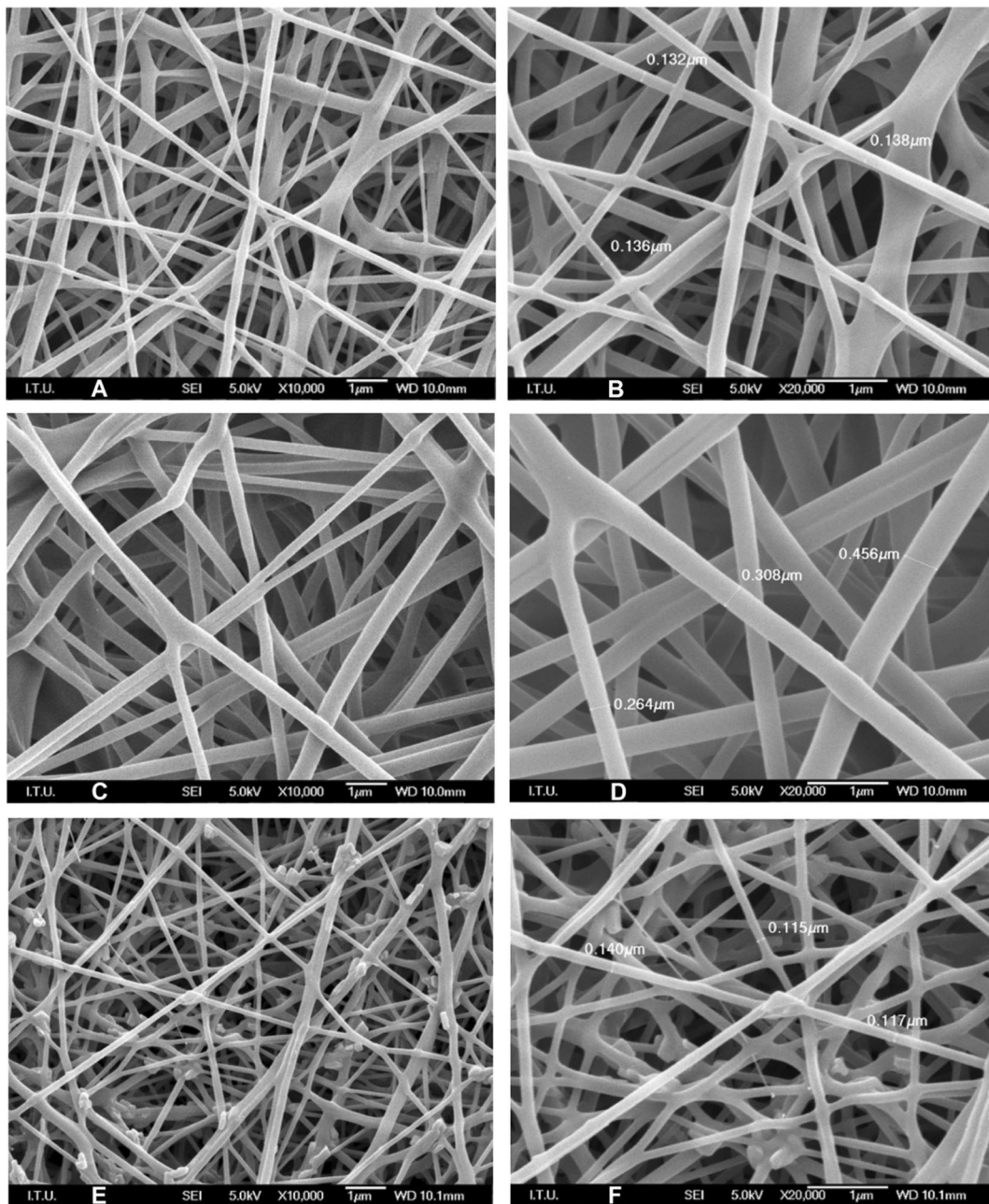


Fig. 4 SEM images of **a** pure PVA, **b** PVA/MA, and **c** PVA/MA/ATM NFm

Adsorption isotherm experiments were conducted with different initial metal ion concentrations diluted from the main solution. One hundred milliliters of the solutions and 100 mg of PVA/MA/ATM NFm were placed in each of four flasks for 480 min at different temperatures (25–45 °C) and at 600 rpm.

Table 2 Physical and thermal properties of nanofiber membrane

Nanofiber membrane	Surface area, m ² /g	Nanofiber diameter, nm	T ₁ , °C	T ₂ , °C	Char, %
PVA/MA/ATM NFm	228.4	115–140	265	453	2.68

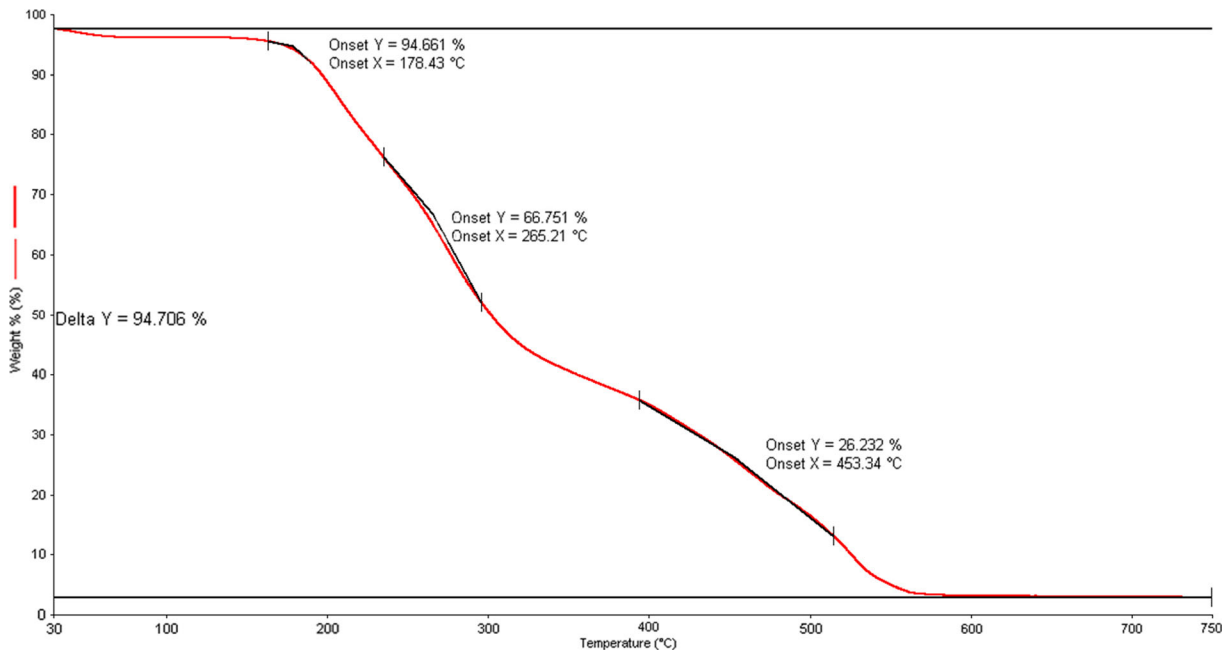


Fig. 5 Thermogram of PVA/MA/ATM NFm

The final experimental series investigated the adsorption kinetics and thermodynamics. The adsorption percentage was calculated using the following equation:

$$\text{Adsorption, \%} = \left[\frac{c_0 - c_t}{c_0} \right] 100 \quad (1)$$

in which c_0 and c_t (mg/L) are the metal ions' concentrations present in the solution before and after adsorption, respectively.

Fig. 6 Effect of pH for adsorption of Pt and Pd on PVA/MA/ATM NFm (480 min, 25 °C, 600 rpm, 3 mg/mL of adsorbent)

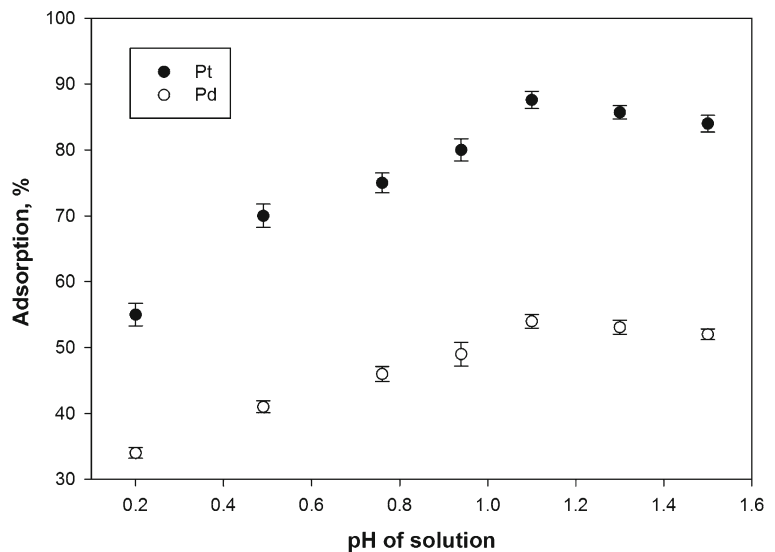
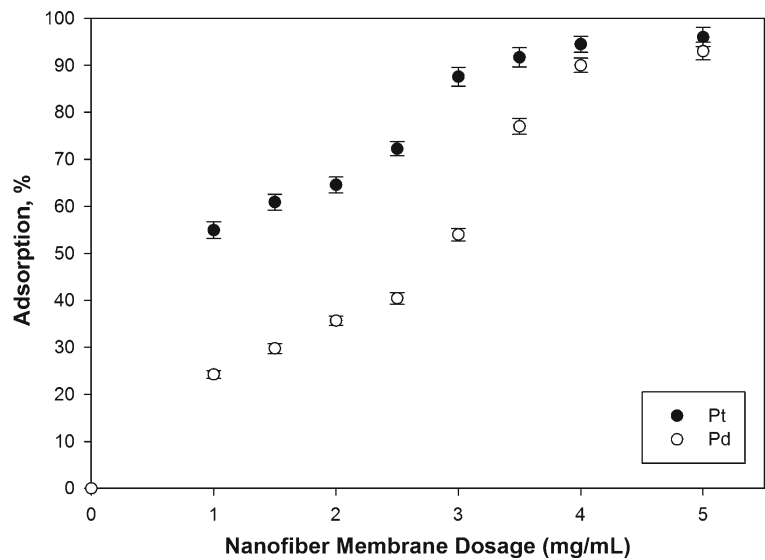


Fig. 7 The effect of the nanofiber membrane dosage on Pt and Pd adsorption (60 min, 25 °C, 600 rpm, pH 1.1, 50 mL of the solution)



2.7 Recovery and Reusage Studies

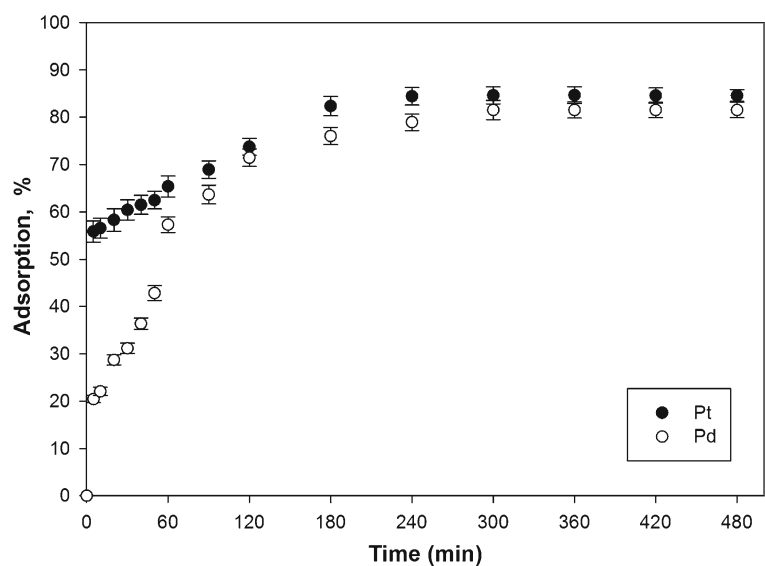
The reusability is very important for nanofiber membranes to be used as adsorbent due to their economical aspects. The ability of the nanofiber membranes to be regenerated and reused provides economic benefits. For this reason, the reusability of the NFM was tested. Desorption experiments were carried out with varying concentrations of (0.5–2.0 M) HCl, (0.5–2.0 M) TU, 0.5 M HCl–1.0 M TU, and 1.0 M HCl–1.0 M TU. The Pt(IV) and Pd(II) ions loaded onto PVA/MA/ATM NFM was washed with deionized water several times and introduced into 25 mL of desorption solutions. The

solutions were vigorously stirred on a magnetic stirrer at 600 rpm at 25 °C for 120 min. The concentration of metal ions released from the PVA/MA/ATM NFM into the aqueous phase was analyzed by ICP-MS. In order to examine the potential reusability of PVA/MA/ATM NFM, the first adsorption–desorption cycle was followed by four other cycles using the same NFM batch. The desorption percentage was calculated as follows:

$$\text{Desorption, \%} = \left[\frac{c_d * V_d}{(c_0 - c_t) * V} \right] * 100 \quad (2)$$

Where c_d (mg/L) is the concentration of the solutes in the desorption solutions; V_d (in L) is the volume of the

Fig. 8 The effect of contact time on Pt and Pd adsorption (100-mg nanofiber membrane, 25 °C, 600 rpm, pH 1.1, 100-mL solution)



desorption solution; c_0 and c_t (mg/L) are the metal ions' concentrations present in the solution before and after adsorption; and V is the volume of the solution (in L).

3 Results and Discussion

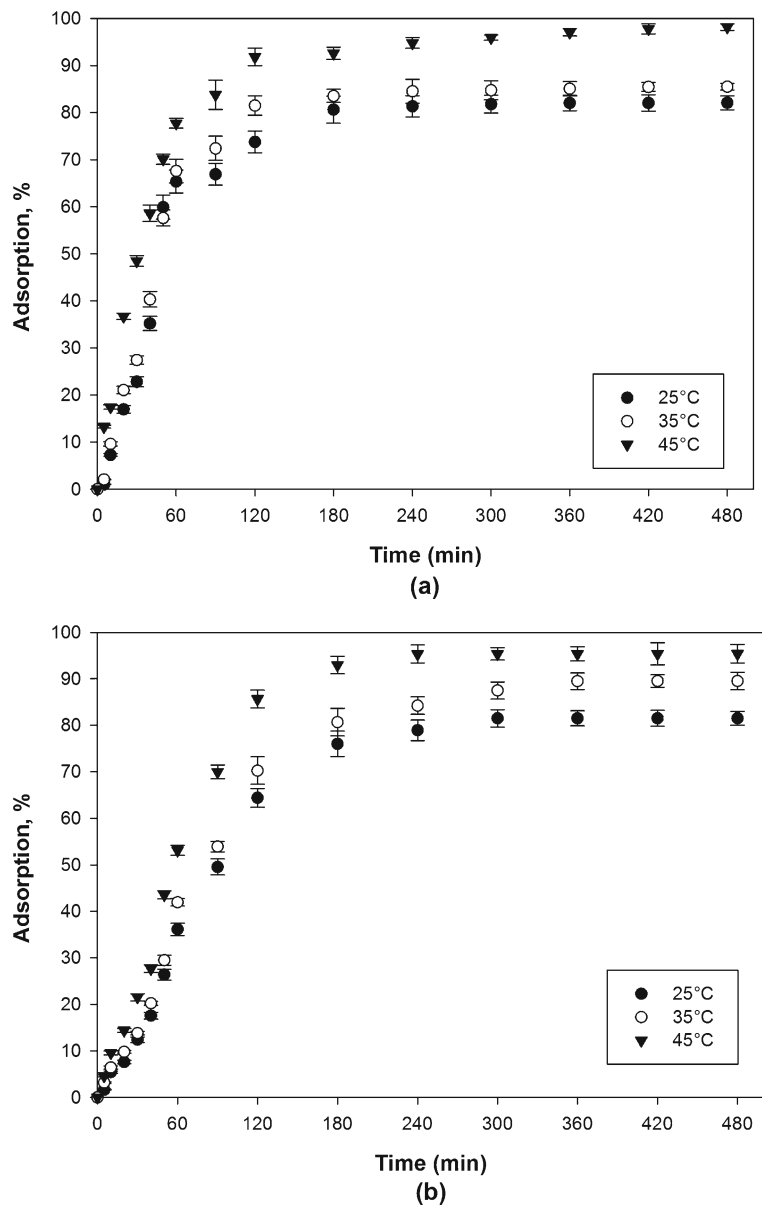
3.1 Characterization of the Nanofiber Membranes

The FT-IR spectrum of ATM is given in Fig. 2. According to the spectrum, the absorption band at 3528 cm^{-1}

can be assigned to the -NH- stretching frequency of the amide group. The carbonyl stretching frequency of the amide group appeared at 1658 cm^{-1} . The C=S group of thioamide shows the band at 1255 cm^{-1} . The peaks at 1086 and 1360 cm^{-1} are attributed to C-N groups. Further, C-H stretching bands are recorded at 2857 and 2928 cm^{-1} . FT-IR spectral measurements confirmed the ATM structure.

PVA/MA NFm at 3325 , 1715 , and 1089 cm^{-1} are attributed to -OH , C=O , and C-O , respectively. Conversely, when the spectrum of PVA/MA/ATM was

Fig. 9 The effect of temperature on **a** Pt and **b** Pd adsorption (50-mg nanofiber membrane, 600 rpm, pH 1.1, 50-mL solution)

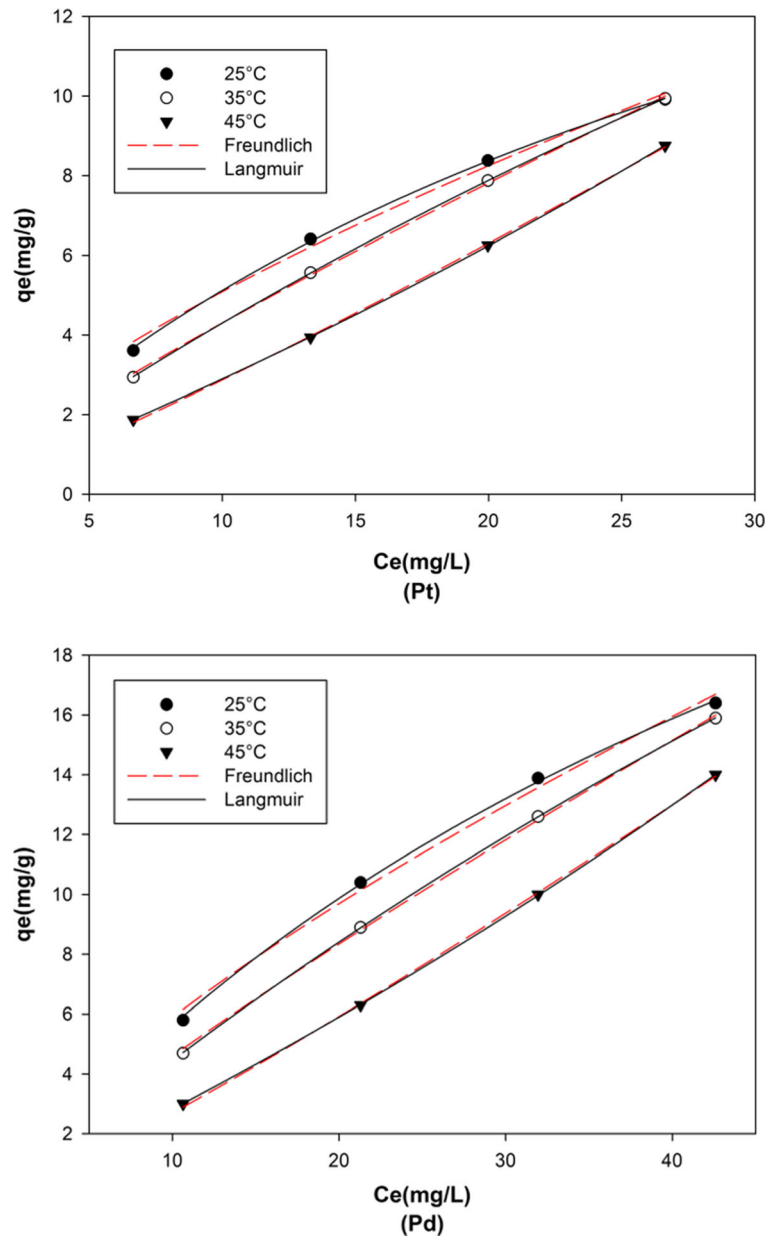


investigated with the spectrum of ATM (see Fig. 2), some peak series showed change. As shown in Fig. 3, the absorption band at 1658 cm^{-1} assigned to C=O bonds, C=S stretching bands at 1255 cm^{-1} , and C–N stretching bands at $1086\text{--}1360\text{ cm}^{-1}$ were shifted to 1661-- , 1247-- , and $1091\text{--}1375\text{ cm}^{-1}$ regions, respectively (Fayemi et al. 2013; Lin and Lien 2013). In Scheme 2, the proposed structure of the PVA/MA/ATM NFm is given.

The SEM images of NFm are shown in Fig. 4. The membranes are composed of numerous, randomly

oriented nanofibers. The pure PVA nanofibers are smooth and uniform, with an average diameter of 135 nm. The PVA/MA NFm has a larger diameter due to increasing the molecular weight (Sill and Von Recum 2008), as their surfaces are still smooth. The average diameter was 260–450 nm. However, there were some beads in the membrane with the introduction of ATM. The average diameter of PVA/MA/ATM nanofibers decreased to 115–140 nm. Furthermore, the surface area was found to be $228.4\text{ m}^2/\text{g}$ by BET analysis (Table 2).

Fig. 10 Adsorption isotherms for Pt and Pd onto the nanofiber membrane at different temperatures (100-mg nanofiber membrane, 600 rpm, 100-mL solution)



The TGA curve reveals the formation of intermediate compounds, which indicates the effect of temperature on the nanofiber formation. As seen in Fig. 5, the thermogram of PVA/MA/ATM nanofiber membrane demonstrated that the nanofiber membrane began to degrade after 100 °C; this may be attributed to the loss of residual water and the unreacted photoinitiator. Moreover, PVA/MA/ATM nanofiber membrane had two stages of decomposition; the first and second decompositions occurred around 265 and 453 °C, respectively, and the char yield at 750 °C was collected and the obtained results were presented in Table 2. Above 453 °C, the weight loss was attributed to main chain scission in the polymer chain and matrices. Therefore, the results indicate that the PVA/MA/ATM NFm is thermally stable at temperatures up to about 453 °C, which is suitable for most of the practical uses.

3.2 The Effect of pH

The pH of a solution is one of the most important parameters for adsorption studies. The adsorption percentage is dependent on the complex form of elements in the solution (i.e., decreasing pH increases the metal ion complex in the solution). Most of the transition metal ions (e.g., Pt, Pd, Au, Rh, etc.) make chloro complexes in a lower pH. However, the solution pH was increased up to 1.5 to easily catch the metal ions in the complex form (Aktas and Morcali 2011b; Morcali et al. 2013c; Morcali et al. 2014b).

When the pH of the solution was adjusted at around pH 1.10, maximum adsorption percentages (about 87 and 54 %) were obtained (Fig. 6) and the Pt and Pd ions

could be quantitatively adsorbed on the sorbent without adding any additional chelating reagent.

3.3 The Effect of the NFm Dosage

The effect of the NFm dosage on Pt and Pd adsorption in the solution was investigated at a contact time of 60 min. In this experiment, PVA/MA/ATM NFm dosage, from 50 to 250 mg per 50-mL solution, resulted in the adsorption of Pt and Pd increasing from 55 to 96 % and from 24 to 93 %, respectively (Fig. 7). With 3.5 mg/mL of PVA/MA/ATM NFm, more than 90 % of Pt(IV) was successfully adsorbed. The adsorption percentage of Pd(II) was adsorbed using 4 mg/mL of PVA/MA/ATM NFm. The adsorption percentage is found to increase with increased dosage because an increased amount of active surface area for binding metal ions is available.

3.4 The Effect of Contact Time

Figure 8 presents the effect of contact time on the adsorption percentage of Pt and Pd by the PVA/MA/ATM NFm in the range of 5 to 480 min. The increased contact time has a positive effect on platinum and palladium adsorption (i.e., the adsorption (%) increases with increased time) and reached equilibrium after 240 and 300 min for Pt and Pd, respectively. Initially, in the first 60 min, the rate of adsorption was higher. Because all the adsorption sites on the nanofiber membrane were vacant and the concentration was high. Then, after approximately 240 min, all the adsorption sites were filled with platinum and palladium ions, resulting in unchanged adsorption percentages. This is an expected

Table 3 Freundlich and Langmuir isotherm constants for the adsorption of Pt and Pd

Pt adsorption				Pd adsorption			
Freundlich isotherm constants							
$T/^\circ\text{C}$	$1/n$	K_F (mg/g)	R^2	$1/n$	K_F (mg/g)	R^2	
25	0.603	0.347	0.9864	0.613	0.261	0.9832	
35	0.817	0.977	0.9891	0.816	0.879	0.9930	
45	1.165	2.825	0.9913	1.081	3.272	0.9896	
Langmuir isotherm constants							
$T/^\circ\text{C}$	Q_{\max} (mg/g)	K_L (L/mg)	R^2	Q_{\max} (mg/g)	K_L (L/mg)	R^2	
25	10.56	0.062	0.9990	18.66	0.004	0.9997	
35	35.97	0.047	0.9999	57.47	0.011	0.9999	
45	69.93	0.039	0.9993	112.36	0.024	0.9993	

result because the adsorption rate of the PVA/MA/ATM NFm was stable.

3.5 The Effect of Temperature

The effect of temperature on Pt and Pd adsorption was studied in the range of 25 to 45 °C in this experimental series, and the percentage adsorption is presented in Fig. 9.

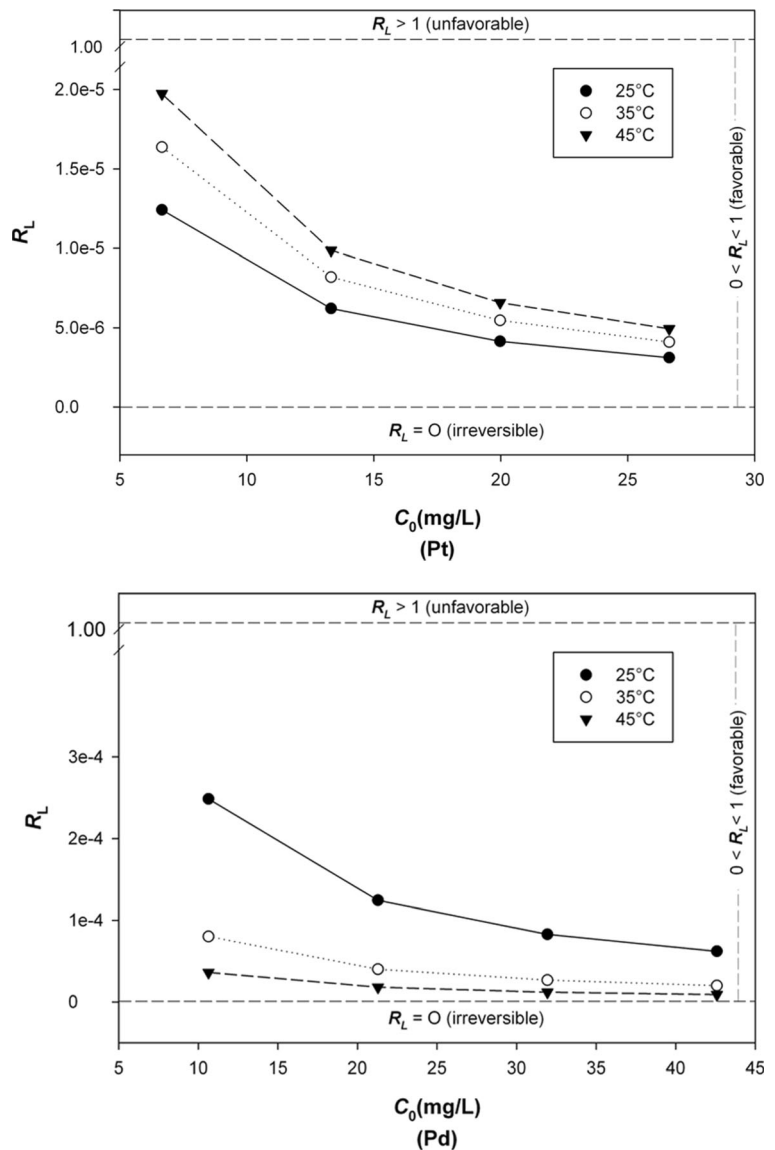
Figure 9 shows that increasing the temperature has a positive effect on Pt(IV) and Pd(II) adsorption for PVA/MA/ATM NFm. After 120 min, an approximately 20 % increment was achieved when the

temperature increased from 25 to 45 °C. The adsorption vs. time curve at 45 °C is continuous, and the percentages of Pt(IV) and Pd(II) reached 98 and 95 %, gradually leading to saturation, which indicates monolayer coverage of metal ions on the surface of the NFm. This was corroborated by the adsorption isothermal studies (Section 3.6).

3.6 Adsorption Isotherms

The adsorption isotherms were investigated in order to describe the adsorption system of the PVA/MA/ATM NFm. The equilibrium data were fitted to the Langmuir

Fig. 11 R_L for the adsorption of Pt(IV) and Pd(II) ions



and Freundlich isotherm models, and their equations are shown below (Foo and Hameed 2010):

$$\frac{c_e}{q_e} = \frac{1}{Q_{\max}K_L} + \frac{1}{Q_{\max}}c_e \quad (3)$$

$$q_e = K_F c_e^{1/2} \quad (4)$$

where q_e is the amount of metal ions adsorbed at equilibrium per unit weight of sorbent (mg/g), Q_{\max} is the monolayer capacity of the adsorbent (mg/g), c_e is the equilibrium ion concentration present in the solution

after adsorption, K_L (L/mg) and K_F (mg/g) are the constants in the Langmuir and Freundlich isotherm models that are related to adsorption capacity, K_L (L/mg) is the constant in the Langmuir isotherm model related to the energy or net enthalpy of adsorption, and n is the constant in the Freundlich isotherm model that measures the adsorption intensity.

In order to determine different isotherms and their correlations with the experimental results, the theoretical plots from each isotherm are shown with the experimental data for the adsorption of Pt(IV) and Pd(II) on PVA/MA/ATM NFM at temperatures from 25 to 45 °C in

Fig. 12 The plot of $\ln(c_0/c_t)$ versus time for Pt and Pd (50 mg, 600 rpm, pH=1.1, 50-mL sol.)

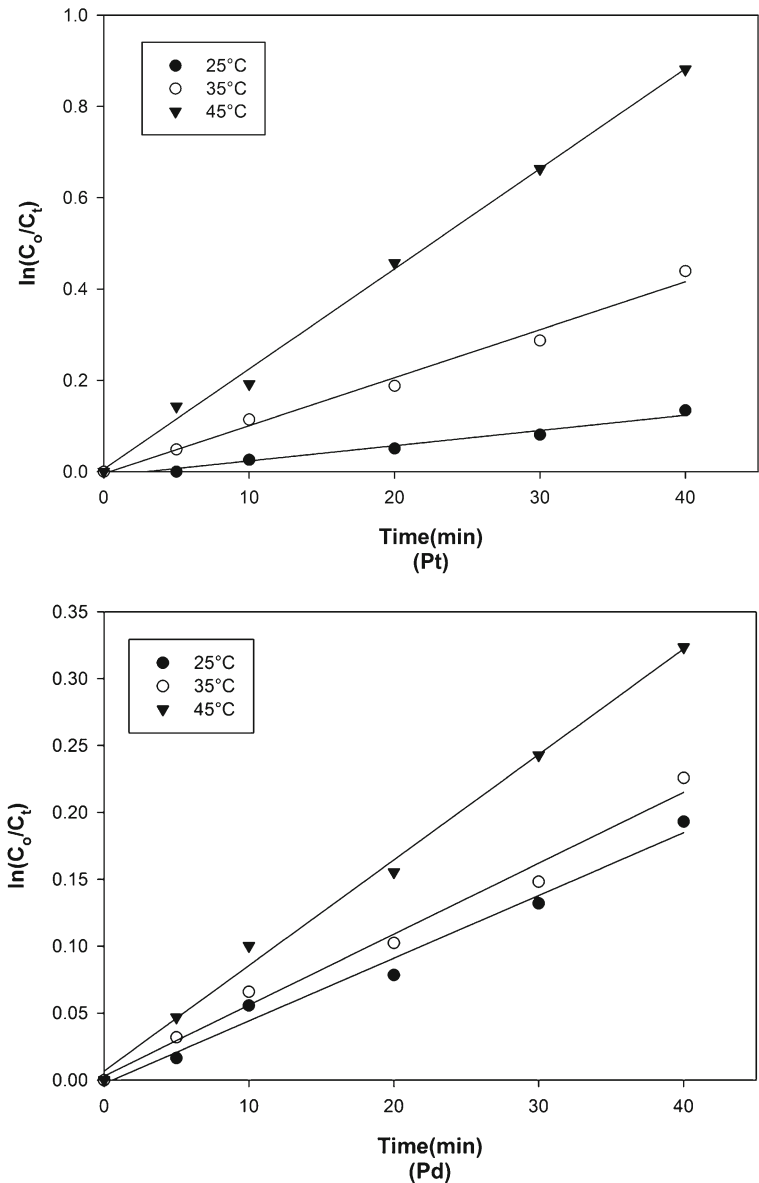


Fig. 13 The Arrhenius plot of $\ln(k)$ versus $1000/T$ Pt and Pd adsorption by PVA/MA/ATM NFm

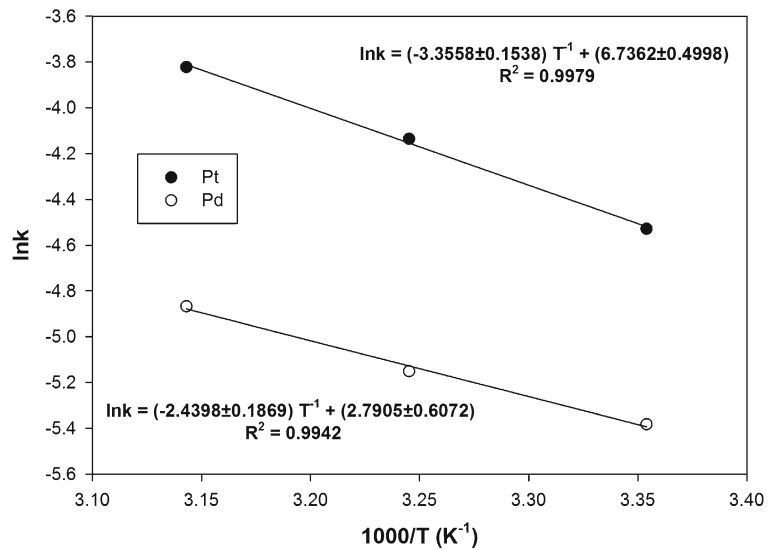


Fig. 10. The graph is plotted in the form of q_e versus c_e . The Langmuir and Freundlich parameters for the adsorption of Pt and Pd ions are listed in Table 3. It is evident from these data that the adsorptions of Pt and Pd ions onto PVA/MA/ATM NFm were a better fit with the Langmuir isotherm model than the Freundlich isotherm model, as indicated by the R^2 values in Table 3. The Langmuir model is the best-known isotherm for describing adsorption from aqueous solution. The Langmuir model assumes that there is no interaction between the adsorbate molecules. The adsorption is localized in a monolayer. The maximum adsorption capacity (Q_{max}) of adsorbent calculated from the Langmuir isotherm equation defines the total capacity of the adsorbent for Pt and Pd ions. The adsorption capacity increases with an increase in the temperature.

Furthermore, the dimensionless separation factor R_L could be calculated by using the Langmuir parameters shown in Table 2. The equation is shown below (Li et al. 2013; Foo and Hameed 2010):

$$R_L = \frac{1}{1 + bc_0} \tag{5}$$

Table 4 Rate constant value for the adsorption of Pt and Pd with respect to temperature

T/K	Pt adsorption			Pd adsorption		
	k (min^{-1})	$\ln k$	E_a (kJ/mol)	k (min^{-1})	$\ln k$	E_a (kJ/mol)
298	0.0108	-4.53	27.90	0.0046	-5.38	20.29
308	0.0160	-4.14		0.0058	-4.15	
318	0.0219	-3.82		0.0077	-4.87	

where b is the Langmuir equilibrium constant (L/mol) and c_0 is the initial concentration. This factor is a criterion of the tendency between the adsorbate and adsorbent. The R_L value is classified into categories including $R_L=0$, $0 < R_L < 1$, and $R_L > 1$, suggesting that adsorption is irreversible, favorable, and unfavorable, respectively. As seen in Fig. 11, the R_L value decreased with increased initial concentrations of Pt(IV) and Pd(II) ions. This shows that platinum and palladium adsorption was more favorable at higher initial concentrations of these precious metal ions.

3.7 Adsorption Kinetics

In this experimental series, several kinetic models (e.g., zero, first, second, third, diffusion model, etc.) were examined in the range of 25 to 45 °C. In order to determine the best-fitting kinetic model, these results were checked against a plot of final concentration versus time. The plot of experimental data was superimposed on them in order to determine which theoretical plot fits the experimental data (plot not shown here).

Table 5 The effect of desorption solutions

Desorption solution	% Desorption	
	Pt	Pd
2.0 M HCl	7.2	6.5
2.0 M TU	56.5	52.8
0.5 M HCl–1.0 M TU	82.1	79.4
1.0 M HCl–1.0 M TU	98.5	97.3

Kinetic studies provide a good fit for Pt and Pd in the first-order ($\ln(c_0/c_t)$), which is described as Eq. (6) (Habashi 1969) and is plotted against time in Fig. 12.

$$kt = \ln\left(c_0/c_t\right) \quad (6)$$

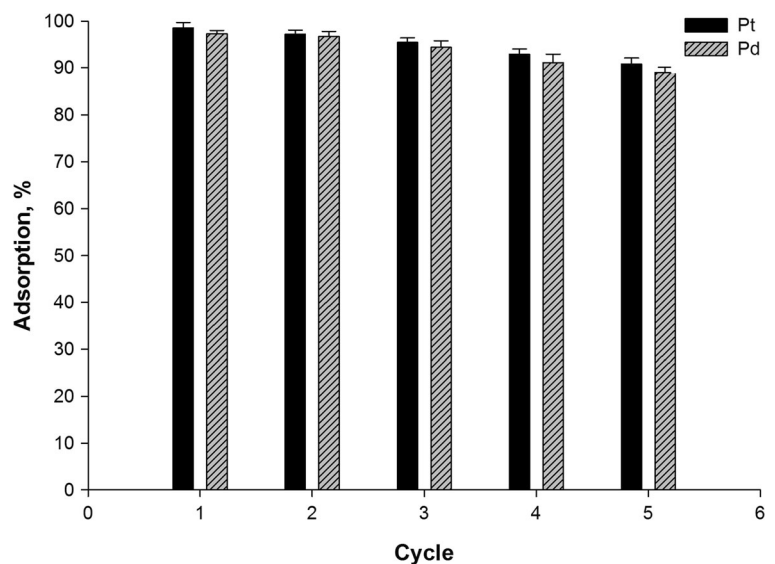
where k is the rate constant, t is the time (min), c_0 is the initial concentration, and c_t is the final concentration.

The activation energy (E_a) was calculated by the Arrhenius equation, according to the following formula (Habashi 1969):

$$k = A e^{-E_a/RT} \text{ or } \ln k = \ln A - E_a/RT \quad (7)$$

where k is the rate constant, E_a is the activation energy, R is the gas constant, and T is temperature (K). Figure 13 displays the Arrhenius plot of $\ln(k)$ versus $1000/T$ for Pt and Pd adsorption. Rate constant values (k) and $\ln(k)$ values with respect to temperature (K) are given in Table 4.

Fig. 14 Desorption and reusability test for PVA/MA/ATM NFm (50-mg loaded nanofiber membrane, 25 °C, 600 rpm, 60 min, 25-mL stripping solution)



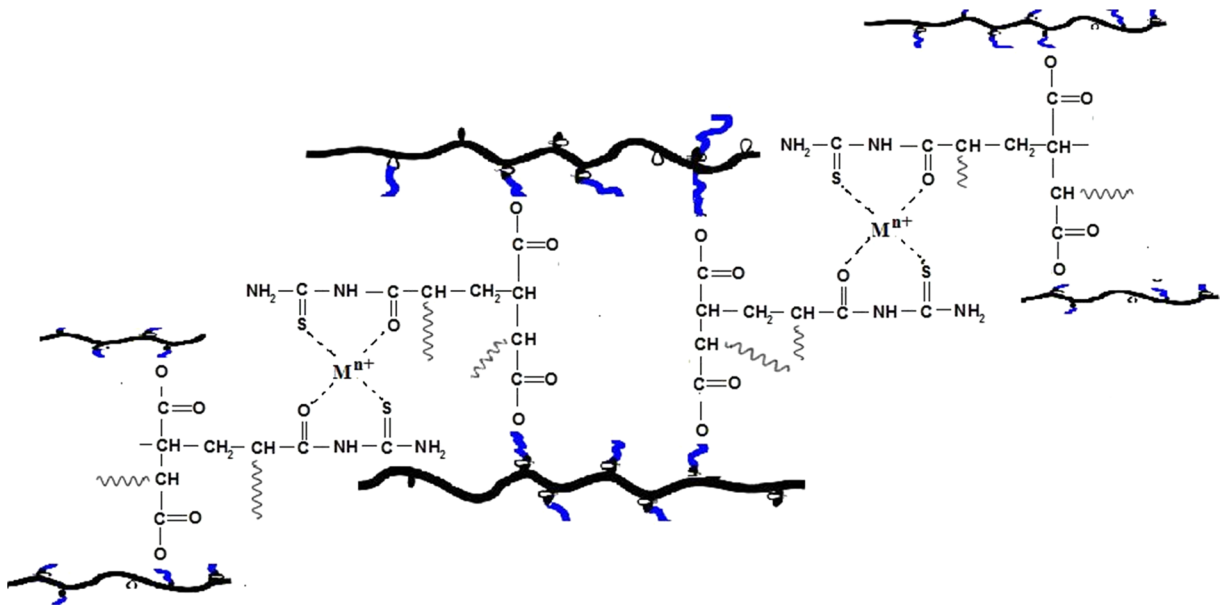
The values of activation energy of the diffusion-controlled processes are low and vary in the range of 4–13 kJ/mol; the values of the activation energy of the chemically controlled process are usually larger than 42 kJ/mol. The reactions controlled by a mixed mechanism (intermediate-controlled process) have activation energy values in the range of 20–35 kJ/mol (Habashi 1969). The activation energy for Pt(IV) and Pd(II) adsorption by PVA/MA/ATM NFm was calculated to be 27.90 and 20.29 kJ/mol, respectively, which is attributed to an intermediate-controlled process for the adsorption of Pt(IV) and Pd(II).

3.8 Recovery and Reusage Studies

This experiment series were carried out with varying concentrations of (0.5–2.0 M) HCl, (0.5–2.0 M) TU, 0.5 M HCl–1.0 M TU, and 1.0 M HCl–1.0 M TU (data are shown Table 5). The results indicated that the 1.0 M HCl–1.0 M TU mixture was the best eluent and obtained the highest desorption ratios. The first desorption ratios were 98.5 % for Pt(IV) and 97.3 % for Pd(II) (see Fig. 14). After five adsorption–desorption cycles of Pt (IV) and Pd (II), the desorption ratios were above 90 %. This result shows that PVA/MA/ATM NFm performs well for repeated use of up to five cycles.

3.9 Adsorption Mechanism

FT-IR and SEM-EDS analyses were used to identify the changes after the adsorption process by indicating the functional groups and their interactions with metal ions.



Scheme 3 Proposal structure of PVA/MA/ATM NFm and metal ions interaction (M^{n+} :Pt(IV), Pd(II))

When PVA/MA/ATM NFm is contacted with the adsorption solution, Pt(IV) and Pd(II) ions are chelate bonded to the sulfur (S) and oxygen (O) atoms of thiourea and carbonyl groups on PVA/MA/ATM NFm surface. Scheme 3 shows a proposed structure of PVA/MA/ATM NFm and metal ion interaction to form a chelated complex.

When the spectrum of Pt/Pd-adsorbed PVA/MA/ATM NFm (Fig. 15) was compared with Fig. 3c, some peak series showed changes. As shown in Fig. 15, the absorption band at 1661 cm^{-1} assigned to C=O bonds and C=S stretching bands at 1247 cm^{-1} were shifted to 1643- and 1226-cm^{-1} regions, respectively. These band

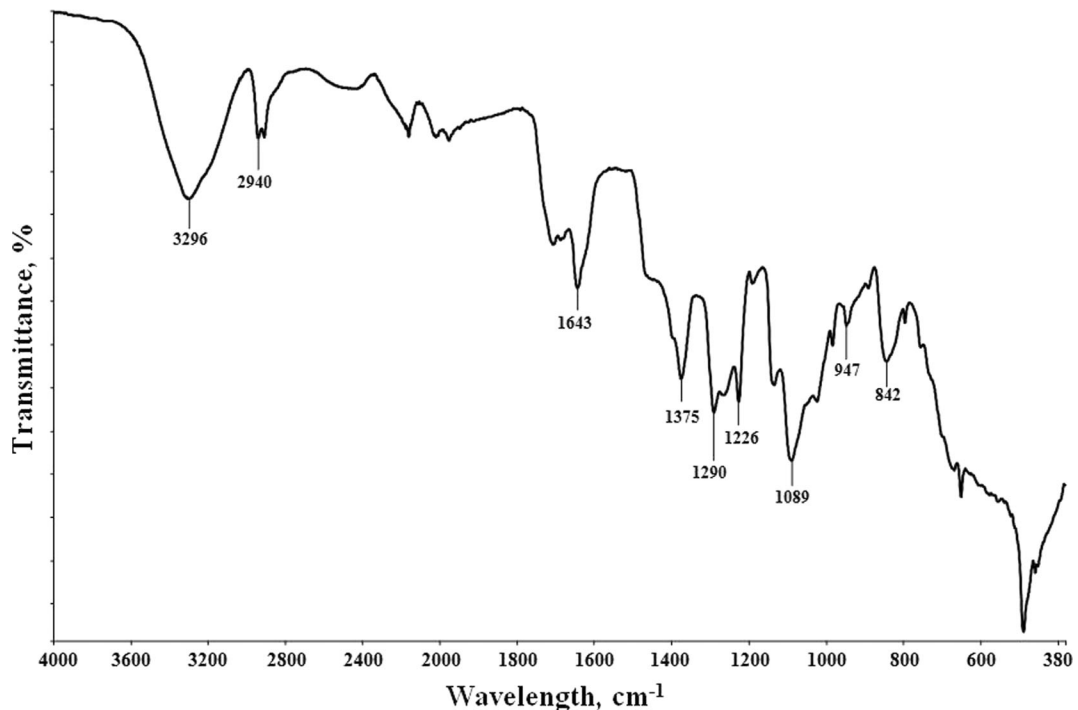


Fig. 15 FT-IR spectra of Pt/Pd-loaded PVA/MA/ATM NFm

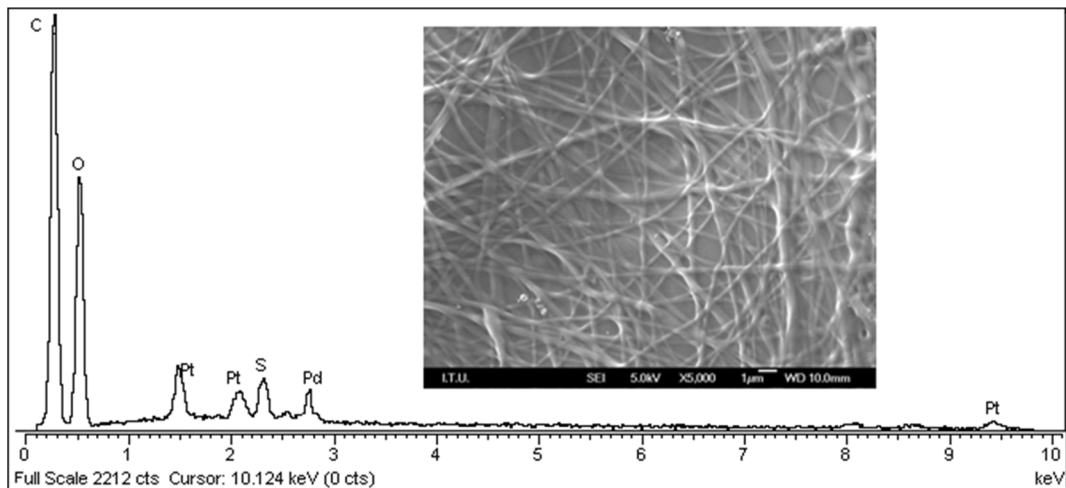


Fig. 16 SEM-EDS image and spectrum of Pt/Pd-loaded PVA/MA/ATM NFm

shifts indicated that the bonded S and O donor atoms play a major role in Pd(II) and Pt(IV) adsorption. Furthermore, Fig. 16 shows the SEM-EDS spectrum energy lines for platinum and palladium, and the SEM-EDS results corroborated the Pt/Pd ions' enrichment on the surface of the specimen. As seen from SEM image, the PVA/MA/ATM NFm of fiber structure was destroyed after using five times for adsorption process.

3.10 Comparison with Other Adsorbents

The comparison of the adsorption capacity of the PVA/MA/ATM NFm with some previously used adsorbent is provided in Table 6. The results showed that PVA/MA/ATM NFm was very effective for the removal of Pt(IV)

and Pd(II) from waste solutions, and the maximum adsorption capacity (Q_{max}) of PVA/MA/ATM NFm was comparable to those of other adsorbents presented in scientific literature (Fujiwara et al. 2007; Peng et al. 2009; Kavaklı et al. 2006; Lin and Lien 2013; Birinci et al. 2009; Fayemi et al. 2013; Morcali et al. 2013b; Morcali et al. 2013b; Morcali et al. 2013c). Maximum adsorption capacity was obtained at lower pH values, and this becomes an advantage, due to the fact that sorbents have no or low affinity for metals, particularly in strong acidic solutions. According to these results, PVA/MA/ATM NFm could be employed as low-cost adsorbents and could be considered as an alternative sorbents for the adsorption of Pt(IV) and Pd(II) from industrial effluents.

Table 6 Comparative data for the adsorption of Pt(IV) and Pd(II) by various adsorbents reported in the literature

Adsorbents	Studied metal	pH	Q_{max} (mg/g)		Reference
			Pt	Pd	
L-lysine-modified crosslinked chitosan resin	Pt(IV), Pd(II), Au(III)	1–2	129.2	109.4	Fujiwara et al. (2007)
Commercial 717 anion-exchange resin	Ag(I), Au(III), Pd(II), Pt(IV)	3	Not reported		Peng et al. (2009)
1,5,9,13-tetrathiacyclohexadecane-3,11-diol anchored poly(p-CMS-DVB) microbeads	Au(III), Ag(I), Pt(IV), Pd(II)	0.5	595	230	Kavaklı et al. (2006)
Thiourea-modified magnetic magnetite nanoparticle (MNP-Tu)	Pt(IV), Pd(II), Au(III)	2	43.3	111.6	Lin & Lien (2013)
Melamine–formaldehyde–thiourea (MFT) resin	Pd(II)	4	15.3		Birinci et al. (2009)
Polystyrene-based nanofibers	Pt(IV), Pd(II)	7.4	4.3		Fayemi et al. (2013)
Lewatit TP 214	Pt(IV)		33.2		Morcali et al. (2013b)
Carbonized pistachio nut shells	Pt(IV)		38.3		Morcali et al. (2013b)
Carbonized rice husk	Pt(IV)		42.0		Morcali et al. (2013c)
PVA/MA/ATM NFm	Pt(IV), Pd(II)	1.1	112	69	This study

4 Conclusions

In this study, in situ photo-cross-linked electrospun PVA-based NFm containing thioamide groups were synthesized by a combination of UV radiation and an electrospinning process. The surface area and nanofiber diameters of PVA/MA/ATM NFm were 228.4 m²/g and 115–140 nm, respectively, and the membrane had good thermal resistance. PVA/MA/ATM NFm showed an efficient adsorption for Pt(IV) and Pd(II) ions. The kinetic of the adsorption was found to follow the first-order rate equation. The Pt(IV) and Pd(II) adsorption by the NFm was an intermediate-controlled process and had activation energies of 27.90 and 20.29 kJ/mol, respectively. By comparing the coefficient of determination using the non-linear method, we found that the Langmuir isotherms had higher coefficients of determination than that of the Freundlich isotherm. The maximum adsorption capacity (Q_{\max}) calculated from the Langmuir isotherm model of PVA/MA/ATM NFm for Pt(IV) and Pd(II) was 69.93 and 112.36 mg/g at 45 °C, respectively. The reusability of NFm was determined after five adsorption–desorption cycles. Consequently, this PVA/MA/ATM NFm is a promising candidate for recovering precious metal ions in aqueous solutions.

Acknowledgments This study is Bihter Zeytuncu's PhD dissertation at Istanbul Technical University. The authors wish to thank Istanbul Technical University for the financial support under BAP project 36460.

Grateful acknowledgements are given to Associate Prof. M. Vezir Kahraman and Dr. Emrah Cakmakci, Marmara University, for providing the electrospinning equipment and ATR-FT-IR analysis and Prof. Dr. Gültekin Göller, Technician Hüseyin Sezer and Talat Alpak Istanbul Technical University, for the SEM analysis.

References

- Aktas, S. (2012). Cementation of rhodium from waste chloride solutions using copper powder. *International Journal of Mineral Processing*, 114–117, 100–105.
- Aktas, S., & Morcali, M. H. (2011a). Platinum recovery from dilute platinum solutions using activated carbon. *Transactions of Nonferrous Metals Society of China*, 21(11), 2554–2558.
- Aktas, S., & Morcali, M. H. (2011b). Gold uptake from dilute chloride solutions by a Lewatit TP 214 and activated rice husk. *International Journal of Mineral Processing*, 101(1–4), 63–70.
- Aliabadi, M., Irani, M., Ismaeili, J., Piri, H., & Parnian, M. J. (2013). Electrospun nanofiber membrane of PEO/Chitosan for the adsorption of nickel, cadmium, lead and copper ions from aqueous solution. *Chemical Engineering Journal*, 220, 237–243.
- Atia, A. A., Donia, A. M., & Yousif, A. M. (2005). Comparative study of the recovery of silver(I) from aqueous solutions with different chelating resins derived from glycidyl methacrylate. *Journal of Applied Polymer Science*, 97(3), 806.
- Aussawasathien, D., Dong, J. H., & Dai, L. (2005). Electrospun polymer nanofiber sensors. *Synthetic Metals*, 154(1–3), 37–40.
- Birinci, E., Gülfein, M., & Aydın, A. O. (2009). Separation and recovery of palladium(II) from base metal ions by melamine-formaldehyde-thiourea (MFT) chelating resin. *Hydrometallurgy*, 95(1–2), 15–21.
- Bolto, B., Tran, T., Hoang, M., & Xie, Z. (2009). Crosslinked poly(vinyl alcohol) membranes. *Progress in Polymer Science*, 34(9), 969–981.
- Borbély, G., & Nagy, E. (2009). Removal of zinc and nickel ions by complexation–membrane filtration process from industrial wastewater. *Desalination*, 240(1–3), 218–226.
- Cakmakci, E., Gungor, A., Kayaman-Apohan, N., Kuruca, S. E., Cetin, M. B., & Dar, K. A. (2012). Cell growth on in situ photo-cross-linked electrospun acrylated cellulose acetate butyrate. *Journal of Biomaterials Science, Polymer Edition*, 23(7), 887–899.
- Fayemi, O. E., Ogunlaja, A. S., Kempgens, P. F. M., Antunes, E., Torto, N., Nyokong, T., et al. (2013). Adsorption and separation of platinum and palladium by polyamine functionalized polystyrene-based beads and nanofibers. *Minerals Engineering*, 53, 256–265.
- Feng, Q., Bi, S., Wang, X., Wei, Q., Hou, D., Huang, X., et al. (2011). Surface modification of electrospun PAN nanofibers and its application for adsorption of lead ions. *Journal of Fiber Bioengineering and Informatics*, 4(4), 383–388.
- Fırlak, M., Kahraman, M. V., Yetimoğlu, E. K., & Zeytuncu, B. (2013). Adsorption of Ag (I) ions from aqueous solutions using photocured thiol-ene hydrogel. *Separation Science and Technology*, 48(18), 2860–2870.
- Foo, K. Y., & Hameed, B. H. (2010). Insights into the modeling of adsorption isotherm systems. *Chemical Engineering Journal*, 156(1), 2–10.
- Fujiwara, K., Ramesh, A., Maki, T., Hasegawa, H., & Ueda, K. (2007). Adsorption of platinum (IV), palladium (II) and gold (III) from aqueous solutions onto l-lysine modified crosslinked chitosan resin. *Journal of Hazardous Materials*, 146, 39–50.
- Gibson, P., Schreuder-Gibson, H., & Rivin, D. (2001). Transport properties of porous membranes based on electrospun nanofibers. *Colloids and Surfaces A: Physicochemical and Engineering Aspects*, 187, 469–481.
- Godlewska-Żyłkiewicz, B., Leńniewska, B., Gaśiewska, U., & Hulanicki, A. (2000). Ion-exchange preconcentration and separation of trace amounts of platinum and palladium. *Analytical Letter*, 33(13), 2805–2820.
- Habashi, F. (1969). *Principles of extractive metallurgy*. USA.: CRC Press.
- Huang, Z. M., Zhang, Y. Z., Kotaki, M., & Ramakrishna, S. (2003). A review on polymer nanofibers by electrospinning and their applications in nanocomposites. *Composites Science and Technology*, 63(15), 2223–2253.

- Hung, N. T., Watanabe, M., & Kimura, T. (2007). Solvent extraction of palladium(II) with various ketones from nitric acid medium. *Solvent Extraction and Ion Exchange*, 25(3), 407–416.
- Islam, M. S., & Karim, M. R. (2010). Fabrication and characterization of poly(vinyl alcohol)/alginate blend nanofibers by electrospinning method. *Colloids and Surfaces A: Physicochemical and Engineering Aspects*, 366(1–3), 135–140.
- Kavakli, C., Malcı, S., Tuncel, S. A., & Salih, B. (2006). Selective adsorption and recovery of precious metal ions from geological samples by 1,5,9,13-tetrathiacyclohexadecane-3,11-diol anchored poly(p-CMS-DVB) microbeads. *Reactive & Functional Polymers*, 66, 275–285.
- Kenawy, E. R., Bowlin, G. L., Mansfield, K., Layman, J., Simpson, D. G., Sanders, E. H., et al. (2002). Release of tetracycline hydrochloride from electrospun poly(ethylene-co-vinylacetate), poly(lactic acid), and a blend. *Journal of Controlled Release*, 81, 57–64.
- Kyzas, G. Z., Kostoglou, M., Lazaridis, N. K., & Bikiaris, D. N. (2013). N-(2-Carboxybenzyl) grafted chitosan as adsorptive agent for simultaneous removal of positively and negatively charged toxic metal ions. *Journal of Hazardous Materials*, 244–245, 29–38.
- Li, X., Zhang, C., Zhao, R., Lu, X., Xu, X., Jia, X., et al. (2013). Efficient adsorption of gold ions from aqueous systems with thioamide-group chelating nanofiber membranes. *Chemical Engineering Journal*, 229, 420–428.
- Lin, T. L., & Lien, H. L. (2013). Effective and selective recovery of precious metals by thiourea modified magnetic nanoparticles. *International Journal of Molecular Sciences*, 14(5), 9834–9847.
- Ma, Z., Masaya, K., & Ramakrishna, S. (2006). Immobilization of Cibacron blue F3GA on electrospun polysulphone ultra-fine fiber surfaces towards developing an affinity membrane for albumin adsorption. *Journal of Membrane Science*, 282(1–2), 237–244.
- Morcali, M. H., Zeytuncu, B., & Yucel, O. (2013a). Rhodium cementation from spent plating solution using Taguchi's method. *Canadian Metallurgical Quarterly*, 52(4), 488–491.
- Morcali, M. H., Zeytuncu, B., Aktas, S., Yucel, O., & Gulluoglu, A. N. (2013b). Platinum adsorption from chloride media using carbonized biomass and commercial sorbent. *Minerals & Metallurgical Processing Journal*, 30, 129–136.
- Morcali, M. H., Zeytuncu, B., & Yucel, O. (2013c). Platinum uptake from chloride solutions using biosorbents. *Materials Research*, 16, 528–538.
- Morcali, M.H., Akman, S. & Yucel, O. (2014a). Determination of the optimum NiS fire assay parameters for Pt, Pd and Rh in automotive exhaust catalytic converters. *Chemical Engineering Communications*, <http://dx.doi.org/10.1080/00986445.2014.907569>.
- Morcali, M. H., Zeytuncu, B., Akman, S., & Yucel, O. (2014b). Sorption of gold from electronic waste solutions by a commercial sorbent. *Chemical Engineering Communications*, 201, 1041–1053.
- Navarro, P., Vargas, C., Alonso, M., & Alguacil, F. J. (2006). The adsorption of gold on activated carbon from thiosulfate-ammoniacal solutions. *Gold Bulletin*, 39(3), 93–97.
- Neghlani, P. K., Rafizadeh, M., & Taromi, F. A. (2011). Preparation of aminated-polyacrylonitrile nanofiber membranes for the adsorption of metal ions: comparison with microfibers. *Journal of Hazardous Materials*, 186(1), 182–189.
- Pearson, R. G. (1963). Hard and soft acids and bases. *Journal of the American Chemical Society*, 85(22), 3533–3539.
- Peng, L., Guang-feng, L., Dalin, C., Shao-yi, C., & Ning, T. (2009). Adsorption properties of Ag(I), Au(III), Pd(II) and Pt(IV) ions on commercial 717 anion-exchange resin. *Transactions of Nonferrous Metals Society of China*, 191, 509–513.
- Ramakrishna, S., Fujihara, K., Teo, W. E., Yong, T., Ma, Z., & Ramaseshan, R. (2006). Electrospun nanofibers: solving global issues. *Materials Today*, 9(3), 40–50.
- Reneker, D. H., & Yarin, A. L. (2008). Electrospinning jets and polymer nanofibers. *Polymer*, 49(10), 2387–2425.
- Sasipriya, K., Suriyaprabha, R., Prabu, P., & Rajendran, V. (2013). Synthesis and characterisation of polymeric nanofibers poly(vinyl alcohol) and poly(vinyl alcohol)/silica using indigenous electrospinning set up. *Materials Research*, 16(4), 824–830.
- Shamsipur, M., Ramezani, M., & Sadeghi, M. (2009). Preconcentration and determination of ultra trace amounts of palladium in water samples by dispersive liquid-liquid microextraction and graphite furnace atomic absorption spectrometry. *Microchimica Acta*, 166(3–4), 235–242.
- Shen, S., Pan, T., Liu, X., Yuan, L., Wang, J., Zhang, Y., et al. (2010). Adsorption of Rh(III) complexes from chloride solutions obtained by leaching chlorinated spent automotive catalysts on ion-exchange resin Diaion WA21J. *Journal of Hazardous Materials*, 179(1–3), 104–112.
- Shen, S., Guishen, L., Pan, T., He, J., & Guo, Z. (2011). Selective adsorption of Pt ions from chloride solutions obtained by leaching chlorinated spent automotive catalysts on ion exchange resin Diaion WA21J. *Journal of Colloid and Interface Science*, 364(2), 482–489.
- Sill, T. J., & Von Recum, H. A. (2008). Electrospinning: applications in drug delivery and tissue engineering. *Biomaterials*, 13, 1989–2006.
- Teng, M., Wang, H., Li, F., & Zhang, B. (2011). Thioether-functionalized mesoporous fiber membranes: sol-gel combined electrospun fabrication and their applications for Hg²⁺ removal. *Journal of Colloid and Interface Science*, 355(1), 23–28.
- Tonnesen, H. H., & Karlsen, J. (2002). Alginate in drug delivery systems. *Drug Development and Industrial Pharmacy*, 28(6), 621–630.
- Trivunac, K., & Stevanovic, S. (2006). Removal of heavy metal ions from water by complexation-assisted ultrafiltration. *Chemosphere*, 64(3), 486–491.
- Wang, H., Li, C., Bao, C., Liu, L., & Liu, X. (2011). Adsorption and determination of Pd(II) and Pt(IV) onto 3'-nitro-4-amino azobenzene modified chitosan. *Journal of Chemical & Engineering Data*, 56(11), 4203–4207.
- Wu, S., Li, F., Wang, H., Fu, L., Zhang, B., & Li, G. (2010a). Effects of poly(vinyl alcohol) (PVA) content on preparation of novel thiol-functionalized mesoporous PVA/SiO₂ composite nanofiber membranes and their application for adsorption of heavy metal ions from aqueous solution. *Polymer*, 51(26), 6203–6211.
- Wu, S., Li, F., Wu, Y., Xu, R., & Li, G. (2010b). Preparation of novel poly(vinyl alcohol)/SiO₂ composite nanofiber

- membranes with mesostructure and their application for removal of Cu(2+) from waste water. *Chemical Communications*, 46(10), 1694–1696.
- Yang, E., Qin, X., & Wang, S. (2008). Electrospun crosslinked polyvinyl alcohol membrane. *Materials Letters*, 62(20), 3555–3557.
- You, Y., Min, B. M., Lee, S. J., Lee, T. S., & Park, W. H. (2005). In vitro degradation behavior of electrospun polyglycolide, polylactide, and poly(lactide-co-glycolide). *Journal of Applied Polymer Science*, 95(2), 193–200.